https://dx.doi.org/10.4314/dujopas.v9i4a.22
ISSN (Print): 2476-8316
ISSN (Online): 2635-3490
Dutse Journal of Pure and Applied Sciences (DUJOPAS), *Vol. 9 No. 4a December 2023*

Adsorptive Removal of Selected Toxic Metals from Pharmaceutical Wastewater using Fe_3O_4/ZnO Nanocomposite

***John Tsado Mathew, Musah Monday, Yakubu Azeh, Musa Mohammed**

Department of Chemistry,
Ibrahim Badamasi Babangida University
Lapai, Niger State
Nigeria

Email: johntsadom@gmail.com

Abstract

Pharmaceutical wastewater is a major source of environmental contamination, often containing toxic metals that pose significant threats to ecosystems and public health. This study explores the potential of magnetite/zinc oxide (Fe_3O_4/ZnO) nanocomposites prepared using a sol-gel method for the removal of lead, cadmium, and copper ions from pharmaceutical wastewater. The nanocomposite was characterized using X-ray diffraction (XRD), High-resolution scanning electron microscopy (HRSEM)/energy dispersive spectroscopy (EDS) and Fourier transmission infrared spectroscopy (FTIR). The XRD analysis of the nanocomposite identified 2θ (theta), of 31.7°, 34.4°, 36.2°, 47.5°, 56.6°, 62.8°, 66.3°, and 67.9° which correspond to the crystal planes of (100), (002), (101), (102), (110), (103), (200), and (112), respectively. The diffraction peaks associated with Fe_3O_4 at 2θ of 18.02°, 29.4°, and 43.3°, related to the crystal planes of (111), (220), and (400), respectively of the Fe_3O_4 phase. The HRSEM image of the nanocomposite exhibited spherical-shaped structures of Fe_3O_4/ZnO, and some irregular shapes. The effects of the contact time, dosage and temperature on the removal percentage of toxic metal ions were studied. Freundlich and Langmuir isotherm constants and correlation coefficients were determined and the equilibrium process was better described by the Langmuir isotherm. The adsorption process followed a second order kinetics and the thermodynamic parameters showed that the involved process was spontaneous. These findings contribute to the advancement of environmentally friendly technologies for the pharmaceutical industry and the broader field of wastewater remediation.
Keywords: Environmental, Metal, Nanocomposites, Pharmaceutical, Wastewater

INTRODUCTION

Pharmaceutical wastewater represents a significant environmental concern due to the presence of various organic and inorganic contaminants, including heavy metals, which can have adverse effects on aquatic ecosystems and public health. Heavy metals such as lead, cadmium, mercury, copper and chromium are commonly found in pharmaceutical effluents, primarily as byproducts of drug manufacturing processes and as trace impurities in raw materials. These heavy metals are known for their toxic and persistent nature, posing substantial risks to the environment and human well-being (Abo-Alkasem *et al*. 2023; Inobeme *et al*., 2023a).

Efforts to mitigate the environmental impact of pharmaceutical wastewater discharge have gained considerable attention in recent years. Among various treatment methods, adsorption has emerged as an effective and versatile technique for the removal of heavy metals from

**Author for Correspondence*

contaminated water sources. In this context, the development of advanced adsorbents with superior adsorption properties is of paramount importance (Ahmad *et al*., 2023; Inobeme *et al*., 2023b).

Nanocomposites, composed of two or more distinct materials at the nanoscale, have demonstrated exceptional potential as adsorbents for heavy metal removal. Among these nanocomposites, magnetite/zinc oxide (Fe_3O_4/ZnO) is promise due to its unique properties, including high surface area, magnetic responsiveness, and the ability to tailor its surface chemistry for specific adsorption purposes. The combination of these two materials in a nanocomposite structure offers the advantages of both magnetite and zinc oxide, making it an ideal candidate for the removal of heavy metals from pharmaceutical wastewater (Damiri *et al.*, 2022; Mathew *et al*., 2023).

The magnetic properties of magnetite enable easy separation of the adsorbent from the treated water using an external magnetic field, thus simplifying the recovery and reuse of the adsorbent. Additionally, the inherent photocatalytic activity of zinc oxide can facilitate the degradation of organic contaminants often found in pharmaceutical wastewater, further enhancing the efficiency of the treatment process (Adetunji *et al*., 2022; Liu *et al*. 2023).

The successful development and utilization of magnetite/zinc oxide nanocomposites for heavy metal removal in pharmaceutical wastewater have the potential to address both environmental and regulatory concerns in the pharmaceutical industry (Baby *et al*., 2022). By reducing heavy metal discharge and improving water quality, this research contributes to the sustainable management of pharmaceutical effluents and underscores the significance of nanomaterials in environmental remediation efforts. Furthermore, the influence of operational parameters such as pH, initial heavy metal concentration, and contact time will be examined to optimize the removal process (Inobeme *et al*., 2023c; Muntean *et al*. 2023).

This study focuses on the adsorptive removal of selected heavy metals, including lead (Pb), cadmium (Cd), and copper (Cu), from pharmaceutical wastewater using magnetite/zinc oxide nanocomposites. The research aims to assess the adsorption kinetics, isotherms, and mechanisms, as well as the overall performance of the nanocomposite adsorbent in removing these heavy metals.

MATERIALS AND METHODS

Synthesis of ZnO/Fe_3O_4 nanocomposites

The nanocomposite was prepared via a wet impregnation method. 2.0 g of the synthesized ZnO nanoparticles was dissolved in 100 cm^3 de-ionized water and stirred for 1 h in a 250 cm^3 beaker using a magnetic stirrer. Exactly 2.0 g of Fe_3O_4 nanoparticles was added to the resultant solution and further stirred for 1 h. The mixture was oven-dried at 105 ^oC for 24 hr and calcined at 450 ^oC for 3 h. The solid sample was pulverized using ceramic mortar and pestle to obtain a homogeneous and fine particles (Thoda *et al*., 2023).

X-ray diffraction

The synthesized samples was characterized with the aid of the powdered X-ray diffraction (XRD) method to determine the extent of graphitization of the samples. Phase identification of the mineral constituents of the samples was done by the XRD. The powdered sample was placed and clipped on the aluminium rectangular sample holder. The diffractograms was recorded in the 2θ range of 20° to 90° and phase identification was established (Mentor *et al.* 2022).

Scanning electron microscopy–Energy dispersive

The morphology of the as-prepared samples will be determined using scanning electron microscopy (SEM). Exactly 0.05 mg will be sprinkled onto carbon adhesives tape and sputter-coated with Au-Pd using Quorum T15OT Analyzer for 5 min. The microscope will be operated with electron high tension at 5 kV for imaging. Scanning electron microscopy (SEM) equipped with energy dispersive spectroscopy (EDS) will further be used to determine the elemental composition of the synthesized nanoparticles and nanocomposites (Mentor *et al.* 2022).

Fourier transform infrared

Fourier transform infrared spectra (FTIR) of the synthesized samples will be recorded using Perkin-Elmer FTIR spectrometer fitted with a deuterated triglycine sulphate (DTGS) detector covering the frequency range of 500-4000 cm^{-1}. The sample cell will be purged with nitrogen gas throughout data collection to exclude carbon(IV) oxide and water vapour. Ten milligrams (0.01 g) of the dried sample will be dispersed in 200 mg of spectroscopic grade KBr to record the spectra. The sample will be recorded in the range of 500 to 4000 cm^{-1} wavenumber (Mentor *et al.* 2022).

Heavy metal determination

Exactly 50.0 cm^3 of the pharmaceutical wastewater sample was measured into a 100 cm^3 beaker with the addition of 15 cm^3 concentrated trioxonitrate (V) solution and heated on a hot plate for 10 min. The solution was allowed to cool, and then deionized water was added and filtered into a 100 cm^3 volumetric flask using Whatman No 42 filter paper. This was then made up to the mark with deionized water and analysis of toxic metals were determined using AAS (Perkin Elmer 200 Atomic Absorption Spectrophotometer) (Sumaila *et al*. 2016; Adamu *et al*. 2017).

RESULTS AND DISCUSSION

The X-ray diffraction (XRD) pattern depicted in Figure 1 illustrates the characteristic scattering of X-rays when interacting with Fe_3O_4 /ZnOnanocomposites produced through sol-gel techniques. This pattern reveals important information about the atomic arrangement within the nanocomposite's crystalline structure. The XRD analysis identifies specific angles of 2θ (theta), which correspond to the scattering angles of the X-rays. For the ZnO component, distinct diffraction peaks were discerned at angles of 31.7°, 34.4°, 36.2°, 47.5°, 56.6°, 62.8°, 66.3°, and 67.9°. These angles correspond respectively to the crystal planes of (100), (002), (101), (102), (110), (103), (200), and (112) within the ZnO crystalline structure.

Similarly, the diffraction pattern also detected peaks associated with Fe_3O_4 at 2θ of 18.02°, 29.4°, and 43.3°, aligning with the crystal planes of (111), (220), and (400) of the Fe_3O_4 phase. The XRD results of the Fe_3O_4 /ZnOnanocomposites indicate the presence of a spinel ferrite phase in the form of $ZnFe_2O_4$ and Fe_3O_4, as deduced from previous research conducted by Ulya and Taufiq (2019). Remarkably, no peaks corresponding to impurities or other substances were observed in the diffraction pattern. This absence of extraneous peaks underscores the purity of the synthesized nanocomposite.

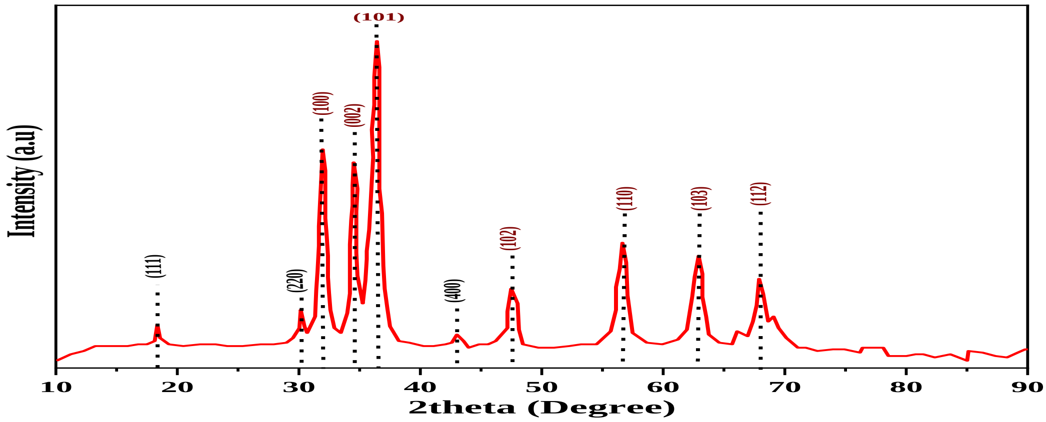

Figure 1: XRD result of Fe_3O_4/ZnO nanocomposites

The structure of the Fe_3O_4/ZnO nanocomposite was examined using SEM. In Figure 2, the visual representation of the Fe_3O_4/ZnO nanocomposite is presented. The nanocomposite exhibits spherical-shaped structures, and some irregular shapes are present within the material. Notably, the most prominent feature of the nanocomposite is the spherical Fe_3O_4/ZnO structure. This spherical structure is beneficial for tissue properties. This advantage stems from the quasi-amorphous arrangement of ZnO nanocrystallites, consistent with the findings from XRD analysis. SEM studied the morphology composition of the Fe_3O_4/ZnO nanocomposite. Figure 2 shows the image of the as-prepared Fe_3O_4/ZnO nanocomposite, which presents spherical-like structures and irregular present in the material. The prominent spherical Fe_3O_4/ZnO nanocomposite has a better effect on tissue properties due to the quasi-amorphous structure of ZnO nanocrystallite by the XRD pattern. The EDX analysis reveals the relative concentrations of Zn, Fe, and O elements, which constitute the primary components of the composite (see Figure 3). The presence of ZnO indicates the incorporation of zinc oxide nanoparticles, while Fe_3O_4 indicates the presence of magnetite nanoparticles.

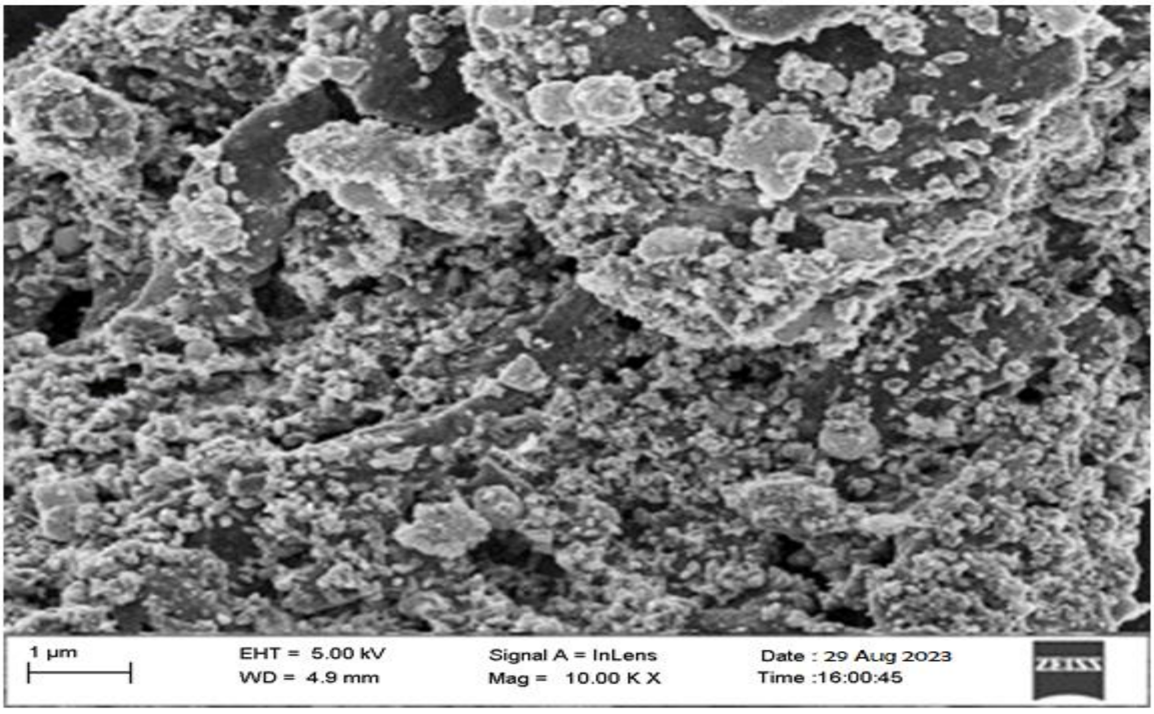

Figure 2: SEM image of Fe_3O_4/ZnO nanocomposites

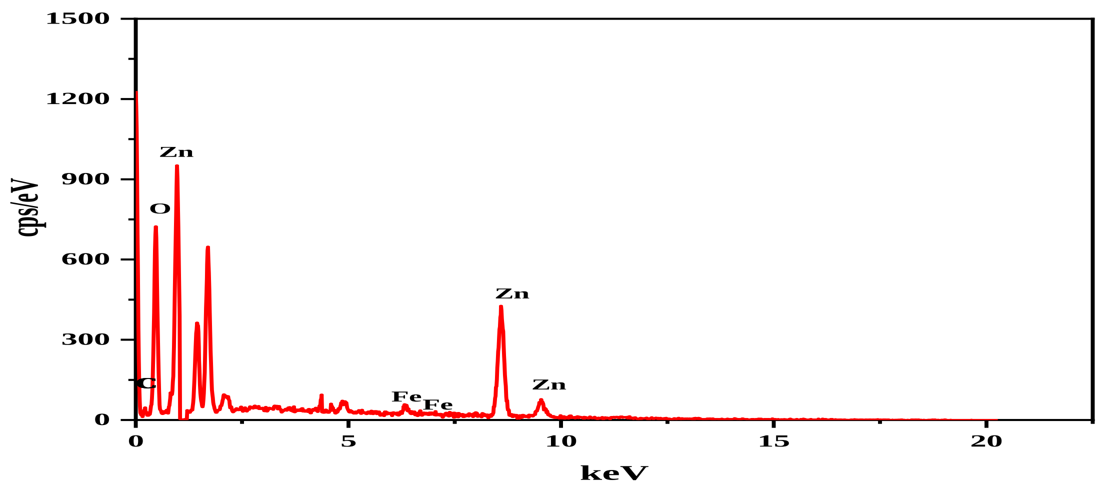

Figure 3: EDX spectrum of Fe_3O_4/ZnO nanocomposites

The FTIR spectrum displayed in Fig. 4 illustrates the distinctive features of the Fe_3O_4/ZnO nanocomposite. The absorbance peaks observed at wavenumbers 3466, 1603, and 1390 cm^{-1} correspond to specific vibration modes associated with the O-H bonds. These vibrations can be attributed to absorbed water molecules and hydroxyl groups on the nanocomposite's surface. Furthermore, a vibration corresponding to the H-O-H bend is noticeable at the wavenumber 1630 cm^{-1}. Distinct vibrations attributed to the carboxyl bonds of symmetric and asymmetric zinc configurations are observed at approximately 1390 cm^{-1} and 1603 cm^{-1}, respectively. These vibrations indicate the involvement of carboxyl groups in the nanocomposite's composition.

The characterization of the Fe-O bond vibrations provides insights into the nanocomposite's structural characteristics. Peaks located at wavenumbers 915 cm^{-1} and 730 cm^{-1} indicate the presence of the Fe_3O_4 spinel structure, confirming the nature of the composite's formation. Additionally, the appearance of a peak at the wavenumber 560 cm^{-1} is linked to the formation of $ZnFe_2O_4$, further confirming the composite's structural makeup.

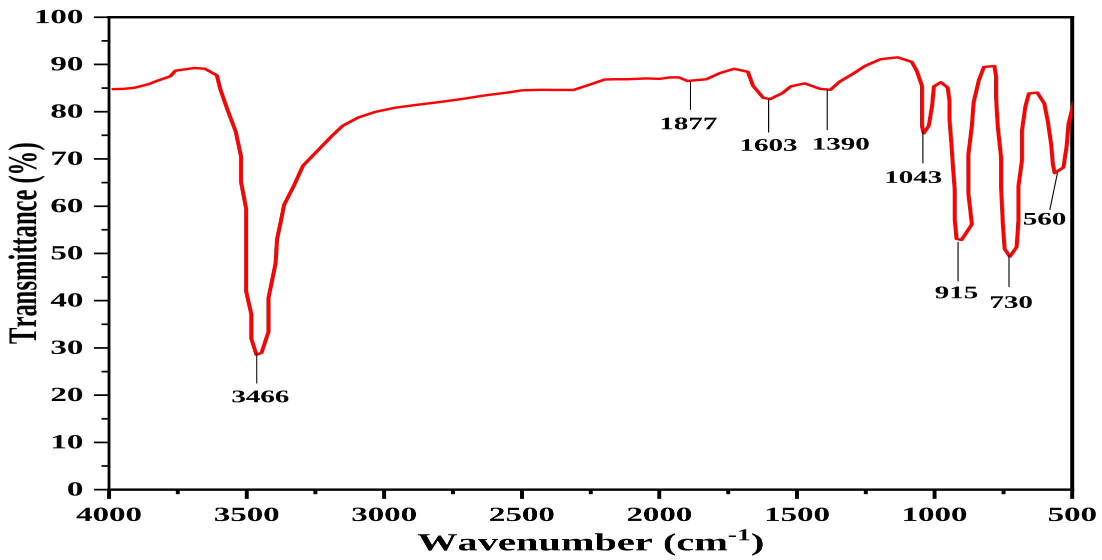

Figure 4: FITR spectrum of Fe_3O_4/ZnO nanocomposites

Batch Adsorption studies

Effect of contact time

Time is crucial in batch adsorption, influencing the adsorbent's interaction with the adsorbate, ensuring optimal removal rates, and enhancing production efficiency. In the conducted adsorption experiment, the adsorbent dosage was set at 0.05 g, and the temperature was maintained at 25 °C. The results, illustrated in Fig. 5, indicate a notable increase in the percentage of metal ion removal. Specifically, the removal rates went from 32.18% to 72.04% for Pb ions, 35.10% to 78.61% for Cd ions, and 38.62% to 80.16% for Cu ions.

The observed trend demonstrates that the efficiency of removing metal ions experiences a rapid rise during the initial stages of adsorption time. This swift increase can be attributed to the substantial available surface area that facilitates the adsorption of metal ions at the start of the process (Jiang *et al*., 2019). The adsorbate rapidly occupies the available adsorption sites as the contact time increases.

Following an optimal duration, the removal rate stabilizes, and additional increments in adsorption time no longer lead to enhanced removal rates. This stabilization occurs because the vacant sites on the nanocomposite become almost entirely occupied, resulting in saturation of the adsorbent. Consequently, the adsorbent's capacity to accommodate additional metal ions diminishes. Subsequently, extending the adsorption time beyond this point does not yield any further improvement in the removal or adsorption of metal ions; instead, it may lead to the release of previously adsorbed ions, a process known as desorption (Batool *et al*., 2023).

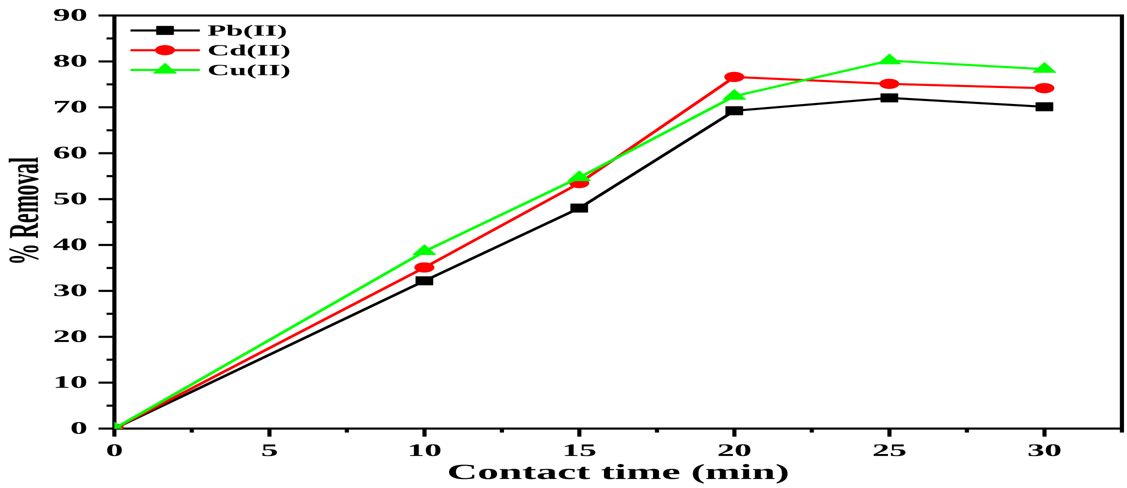

Figure 5: Effect of contact time on the removal of heavy metal ions

Effect of adsorbent dosage

The adsorption dose is a pivotal factor in the wastewater treatment process through adsorption. This parameter significantly influences the adsorption capacity and the efficacy of any substance to capture a specific volume of pollutants. In the context of this study, the researchers focused on the adsorption of Pb(II), Cd(II), and Cu(II) ions from wastewater utilizing a Fe_3O_4/ZnO nanocomposite. They conducted experiments by varying the quantity of this adsorbent, ranging from 0.1 to 0.3 g (as shown in Figure 2). The outcome, presented in

Figure 6, is depicted in terms of the percentage of metal ion removal achieved using the nanocomposite.

Interestingly, the removal efficiency exhibited a range between 78.42% and 98.92% for Pb(II), 82.10% and 99.64% for Cd(II), and 85.10% and 100% for Cu(II) ions, respectively. A noteworthy trend emerged: as the dosage of the adsorbent increased, the rate of metal ion removal also increased. This rapid adsorption behavior implies a strong attraction between the metal ions and the adsorption material, which can be attributed to the specific structural and morphological characteristics of the nanocomposite, as highlighted in a previous study by Lian et al. (2020). The augmentation in the removal rate is closely linked to the rise in available adsorption sites as the adsorbent quantity escalates, as observed and explained in research by Feng *et al*. (2020).

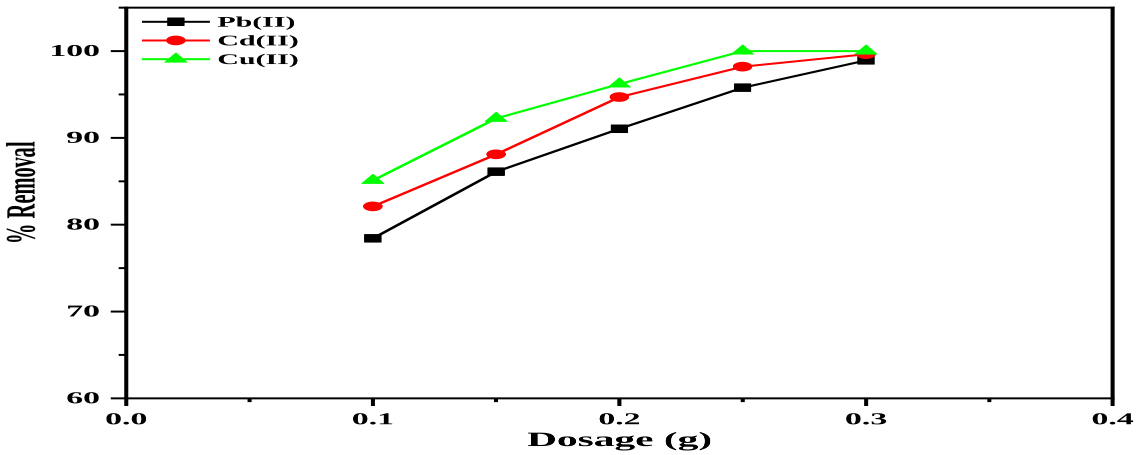

Figure 6: Effect of dosage on the removal of heavy metal ions

Effect of temperature

Figure 7 illustrates the adsorption process for Pb, Cd, and Cu ions using a Fe_3O_4/ZnO nanocomposite. The effectiveness of this process is quantified by the percentage of ions removed from a solution. In specific terms, the removal rates for Pb(II), Cd(II), and Cu(II) ions increased as follows: Pb ions' removal rate rose from 52.30% to 80.40%, Cd ions' removal rate increased from 58.10% to 83.19%, and Cu ions' removal rate elevated from 62.44% to 92.10%. These improvements were observed when the nanocomposite was subjected to higher temperatures. This enhancement can be attributed to the structural characteristics of the nanocomposite under elevated temperatures, as detailed in a study by Wang *et al*. (2021).

One possible explanation for this phenomenon is that the nanocomposite's internal empty spaces became larger, and a greater number of adsorption sites were exposed due to the influence of high temperature (Zaimee *et al*., 2021). As the temperature rises, the mobility of metal ions, such as Cu(II) ions, is heightened. Consequently, more of these ions can migrate and enter the expanded internal voids of the nanocomposite. Moreover, the elevated temperature strengthens the interaction between the adsorbent (nanocomposite) and the sites on which the pollutants (metal ions) are adsorbed. Notably, the findings indicate that the adsorption process between the metal ions and the Fe_3O_4/ZnO nanocomposite is driven by an increase in temperature (endothermic).

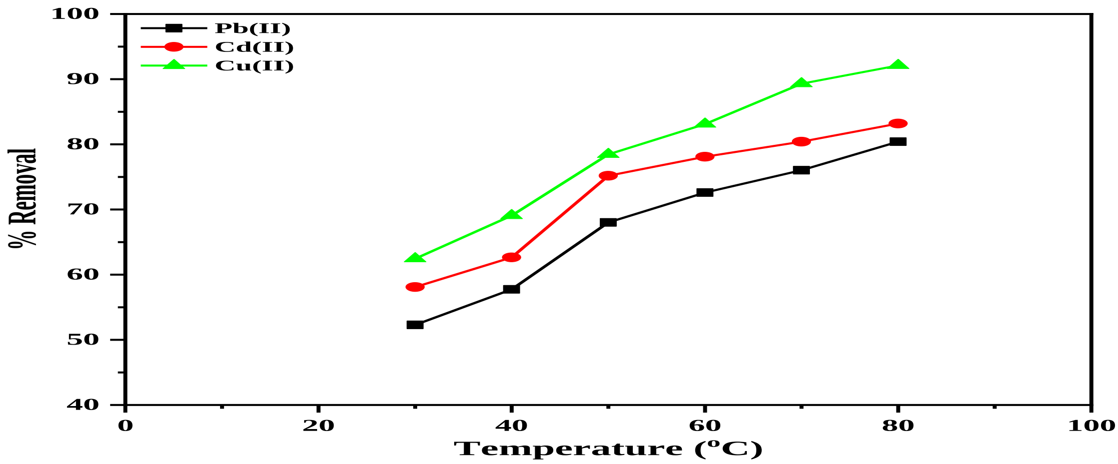

Figure 7: Effect of temperature on the removal of heavy metal ions

Adsorption isotherms

The Langmuir isotherm model is described in Eq. 1 (Langmuir 1918).

$$\frac{C_e}{q_e} = \frac{1}{bq_m} + \frac{C_e}{q_m} \qquad (1)$$

where C_e is the equilibrium concentration of substrates in the solution (mg/dm^3), q_e is the adsorption capacity at equilibrium (mg/g), q_m is the maximum adsorption capacity (mg/g), and b is the adsorption equilibrium constant (L/mg). Values of Langmuir parameters are shown in Table 1. Values of q_{max}, K_L, and regression coefficient (R^2) are listed in Table 1. These values for nanocomposite adsorbent indicated that the Langmuir model describes the adsorption phenomena favourable.

On the other hand, the Freundlich isotherm model is particularly relevant when discussing adsorption on surfaces with varying properties. This model considers the interactions occurring between the molecules being adsorbed. Using the Freundlich equation, it can be inferred that as the sorption centers on the adsorbent become saturated, the energy associated with the sorption process decreases exponentially. This isotherm model is particularly suited for describing systems with diverse surfaces and can be mathematically expressed through Equ. 5, as originally formulated by Freundlich in 1906.

$$\ln q_e = \ln K_f + \frac{1}{n}\ln C_e \qquad (2)$$

where K_f and n are Freundlich constants, n indicates favourable the adsorption process and K_f (mg/g) is the adsorption capacity of the adsorbent

The Freundlich equilibrium constants were established by utilizing the linear form of the Freundlich equation. The parameter "n" in the equation serves as an indicator of the extent of non-linearity between the concentration of the solution and the adsorption process. Specifically, if the value of "n" is 1, it signifies a linear adsorption relationship. On the other hand, if "n" is greater than 1, it implies a non-linear, physical adsorption process. The investigation revealed that the "n" values in the Freundlich equation were determined to be 1.49 for Pb(II), 1.90 for Cd(II), and 194 for Cu(II) ions, as outlined in Table 1. Notably, the "n" values fall from 1 to 10 in this study. This range strongly suggests that the physical adsorption of Pb(II), Cd(II), and Cu(II) ions onto the Fe_3O_4/ZnO nanocomposite is the prevailing mechanism.

Table 1: Isotherm models of metal ions removal in wastewater

Isotherm	Parameter	Pb(II)	Cd(II)	Cu(II)
Langmuir	K_L	0.0051	0.0049	0.0049
	Q_m	93.09	122.86	134.65
	R^2	0.9893	0.9904	0.9991
Freundlich	K_f	0.416	3.091	5.982
	n	0.408	0.642	0.873
	R^2	0.9690	0.9896	0.9901

Adsorption kinetics

Two kinetic models were used to investigate the kinetic behavior of Pb(II), Cd(II), and Cu(II) ion adsorption onto Fe_3O_4/ZnO nanocomposite. The linear equations of the pseudo-first-order (PFO) and pseudo-second-order (PSO) kinetic models are shown in Eqs. (3) and (4), respectively.

$$\ln(q_e - q_t) = \ln q_e - k_1 t \quad (3)$$

$$\frac{t}{q_t} = \frac{1}{k_2 q_e^2} + \frac{1}{q_e} t \quad (4)$$

where q_e and q_t are the amount of metal ion adsorbed per unit mass of the adsorbent (mg/g) at equilibrium time and time t, respectively, k_1 is the pseudo-first-order rate constant and k_2 is the pseudo-second-order rate constant (Musah *et al.*, 2022).

The experimental data was fitted using the PFO and PSO models to determine the appropriate adsorption kinetic parameters (Table 2). As indicated in Table 2, the PSO kinetic model exhibited a superior correlation coefficient value (R^2) when applied to fit the experimental data concerning the adsorption of metal ions onto the Fe_3O_4/ZnO nanocomposite. This suggests that the process of metal ion adsorption onto the Fe_3O_4/ZnO nanocomposite could be primarily influenced by chemical adsorption kinetics. This finding aligns with a study conducted by Shaba *et al*. (2022), focusing on the utilization of Fe_3O_4/ZnO nanocomposite for eliminating Cu(II) and Cr(VI) ions from wastewater originating from petroleum refining.

Table 2: Kinetic models of metal ions removal in wastewater

Kinetic	Parameter	Pb(II)	Cd(II)	Cu(II)
Pseudo-first-order	k_1	0.00226	0.00444	0.00818
	q_e	60.274	78.901	84.418
	R^2	0.8420	0.8785	0.9016
Pseudo-second-order	k_2	0.6919	0.718	0.726
	q_e	103.852	114.710	120.585
	R^2	0.9710	0.9923	0.9991

Thermodynamic study

Thermodynamic parameter for Pb(II), Cd(II) and Cu(II) ions adsorption onto Fe_3O_4/ZnO nanocomposite were determined as shown in Eq. 5-7.

$$K_d = \frac{q_e}{C_e} \quad (5)$$

$$\Delta G = -RT\ln K_d \quad (6)$$

$$\Delta G = \Delta H - T\Delta S \quad (7)$$

where the values of ΔG, ΔH and ΔS were measured in kJ/mol, kJ/mol and J/molK respectively. T is the absolute temperature (K), R is the universal gas constant (8.314 J/molK), K_d value is obtained by plotting $\ln(\frac{q_e}{C_e})$ against C_e. (Shaba *et al.*, 2019)

The provided data in Table 3 presents the computed thermodynamic parameters, namely ΔG°, ΔH°, and ΔS°, related to the adsorption process of Pb(II) and Cd(II) ions onto a Fe_3O_4/ZnO nanocomposite. The observed positive value of ΔS°, ranging from 53.5 to 90.4 J/mol K, indicates an increase in disorder or randomness at the interface between the solid solution and the adsorbed ions during the adsorption process of Pb(II), Cd(II), and Cu(II) ions onto the Fe_3O_4/ZnO nanocomposite. In simpler terms, this suggests that the arrangement of particles becomes less structured as these ions bind to the nanocomposite material.

The fact that the calculated ΔG° has negative values implies that the adsorption process is spontaneous. This means that the ions from the solution are naturally inclined to adhere to the nanocomposite surface without requiring external intervention. This observation aligns with a study conducted by Sahmoune (2019). Furthermore, it's noteworthy that the change in free energy (ΔG°) becomes more negative with increased temperature. This indicates an augmented driving force for the adsorption process as the temperature rises. This could be attributed to a couple of possibilities. One is that as the temperature goes up, more sites on the nanocomposite surface become available for adsorption, effectively enhancing the adsorption capacity. Alternatively, the energy distribution associated with the adsorption sites may follow an exponential pattern, and higher temperatures facilitate overcoming the energy barrier required for adsorption.

Table 3: Thermodynamic study of metal ions removal in wastewater

Parameter	Temperature (°C)	ΔS (kJ/molK)	ΔH (kJ/mol)	ΔG (kJ/mol)
Pb(II)	30	20.24	73.01	-1.88203
	40	20.24	73.01	-2.61213
	50	20.24	73.01	-3.34223
	60	20.24	73.01	-4.07233
	70	20.24	73.01	-4.80243
	80	20.24	73.01	-5.53253
Cd(II)	30	21.15	77.01	-2.18403
	40	21.15	77.01	-2.95413
	50	21.15	77.01	-3.72423
	60	21.15	77.01	-4.49433
	70	21.15	77.01	-5.26443
	80	21.15	77.01	-6.03453
Cu(II)	30	22.30	82.62	-2.73386
	40	22.30	82.62	-3.56006
	50	22.30	82.62	-4.38626
	60	22.30	82.62	-5.21246
	70	22.30	82.62	-6.03866
	80	22.30	82.62	-6.86486

CONCLUSION

This study has provided valuable insights into the potential of nanomaterials for heavy metal removal and its practical applicability in wastewater treatment processes. The findings of this study highlight the promise of magnetite/zinc oxide nanocomposites as efficient adsorbents for heavy metal removal from pharmaceutical wastewater. Furthermore, the potential for simultaneous removal of organic contaminants through photocatalysis adds to the environmental benefits of this treatment approach. In addition, this research underscores the importance of developing advanced materials for the removal of heavy metals from industrial wastewater. The use of nanocomposites, like magnetite/zinc oxide, offers a sustainable and eco-friendly solution for addressing heavy metal pollution concerns in the pharmaceutical sector. The insights gained from this study can inform future efforts in environmental remediation and contribute to the development of innovative technologies for cleaner and safer water resources.

ACKNOWLEDGEMENT
We express our gratitude to the Tertiary Education Trust Fund (TETFund) for funding this study, as well as the management of IBB University, Lapai for creating an environment that encourages research.

REFERENCES
Abo-Alkasem, M.I., Hassan, N.H. and Abo Elsoud, M.M. (2023). Microbial bioremediation as a tool for the removal of heavy metals. *Bulletin of the National Research Centre*, 47, 31.

Adamu A., Iyaka Y. A., Mathew J. T**.**, Inobeme A. and Egharevba H. O. (2017). Assessment of Some Heavy Metal Contamination and analysis of Physicochemical Parameters of Surface Soil within the Vicinity of Minna Railway Station, Niger State, Nigeria. *Journal of Applied Life Sciences International,* 10(1), 1-9.

Adetunji, C. O., Inobeme, A., Olaniyan, O. T., Anani, O. A., Mathew, J. T., Bodunrinde, R. E., Adetunji, J. B. and Hefft, D. I. (2022). Nanomaterials as Effective Tools for Detection and Microbial Diagnosis of Foodborne Pathogens. The Science of Nanomaterials: Basics and Applications. Suresh C. Ameta & Rakshit Ameta (Eds.), Apple Academic Press, Inc. Co-published with CRC Press (Taylor & Francis)

Ahmad, A., Kamaruddin, M. A., H P S, A. K., Yahya, E. B., Muhammad, S., Rizal, S., Ahmad, M. I., Surya, I., and Abdullah, C. K. (2023). Recent Advances in Nanocellulose Aerogels for Efficient Heavy Metal and Dye Removal. *Gels (Basel, Switzerland)*, *9*(5), 416.

Baby, R., Hussein, M. Z., Abdullah, A. H., and Zainal, Z. (2022). Nanomaterials for the Treatment of Heavy Metal Contaminated Water. *Polymers*, *14*(3), 583.

Batool, F., Mohyuddin, A., Amjad, A., ul Hassan, A., Nadeem, S., Javed, M., Othman, M.H.D., Chew, K.W., Rauf, A. and Kurniawan, T.A., 2023. Removal of Cd (II) and Pb (II) from synthetic wastewater using Rosa damascena waste as a biosorbent: An insight into adsorption mechanisms, kinetics, and thermodynamic studies. *Chemical Engineering Science*, *280*, p.119072.

Damiri, F., Andra, S., Kommineni, N., Balu, S. K., Bulusu, R., Boseila, A. A., Akamo, D. O., Ahmad, Z., Khan, F. S., Rahman, M. H., Berrada, M., and Cavalu, S. (2022). Recent Advances in Adsorptive Nanocomposite Membranes for Heavy Metals Ion Removal from Contaminated Water: A Comprehensive Review. *Materials (Basel, Switzerland)*, *15*(15), 5392.

Feng, X., Yu, Z., Long, R., Li, X., Shao, L., Zeng, H., Zeng, G. and Zuo, Y., 2020. Self-assembling 2D/2D (MXene/LDH) materials achieve ultra-high adsorption of heavy metals Ni2+ through terminal group modification. *Separation and Purification Technology*, *253*, p.117525.

Inobeme, A., Adetunji, C. O., Mathew, J. T., Okonkwo, S., Bamigboye, M. O., Ajai, A. I., Afoso, E. and Inobeme, J. (2023)a. Advanced nanotechnology for the degradation of persistent organic pollutants. In: Shah, M. ed. *Microbial Degradation and Detoxification of Pollutants*. Berlin, Boston: De Gruyter, pp. 51-72.

Inobeme, A., Adetunji, C. O., Maliki, M., Onyeachu, B. I., Kelani, T., Eziukwu, C. A., Olori, E., Mathew, J. T., and Bamigboye, M. O. (2023)b. Strategies to synthesize, advantages, and disadvantages of pharmaceutical nanoparticles. In book: Nanotechnology for Drug Delivery and Pharmaceuticals. Academic Press is an imprint of Elsevier, 371-402.

Inobeme, A., Adetunji, C. O., Mathew, J T., Ajai, A. I., Inobeme, J., Bamigboye, M. O., Onyeaku, S., Maliki, M., Eziukwu, C. and Tawa, K. (2023)c. Nanotechnology for Bioremediation of Heavy Metals. In book: Microbial Technologies in Industrial Wastewater Treatment. Springer Nature Singapore, 19-30.

Jiang, D., Yang, Y., Huang, C., Huang, M., Chen, J., Rao, T., and Ran, X. (2019). Removal of the heavy metal ion nickel (II) via an adsorption method using flower globular magnesium hydroxide. *Journal of hazardous materials*, *373*, 131-140.

Lian, Z., Li, Y., Xian, H., Ouyang, X. K., Lu, Y., Peng, X., and Hu, D. (2020). EDTA-functionalized magnetic chitosan oligosaccharide and carboxymethyl cellulose nanocomposite: Synthesis, characterization, and Pb (II) adsorption performance. *International Journal of Biological Macromolecules*, *165*, 591-600.

Liu, M., Ye, Y., Ye, J., Gao, T., Wang, D., Chen, G., and Song, Z. (2023). Recent Advances of Magnetite (Fe3O4)-Based Magnetic Materials in Catalytic Applications. *Magnetochemistry*, *9*(4), 110.

Mathew, J. T., Adetunji, C. O., Inobeme, A., Musah, M., Azeh, Y., Otori, A.A., Shaba, E. Y., Mamman, A. and Tanko, E. (2023). Removal of Heavy Metals Using Bio-remedial Techniques. Springer Nature Switzerland AG 2023 M. P. Shah (ed.), Modern Approaches in Waste Bioremediation, 117-130.

Mentor, S., Cummings, F., and Fisher, D. (2022). Preparation of biological monolayers for producing high-resolution scanning electron micrographs. *PloS one*, *17*(7), e0266943.

Muntean, S. G., Halip, L., Nistor, M. A., and Păcurariu, C. (2023). Removal of Metal Ions via Adsorption Using Carbon Magnetic Nanocomposites: Optimization through Response Surface Methodology, Kinetic and Thermodynamic Studies. *Magnetochemistry*, *9*(7), 163.

Musah, M., Azeh, Y., Mathew, J. T., Umar, M.T., Abdulhamid, Z. and Muhammad, A. I. (2022). Adsorption Kinetics and Isotherm Models: A Review. Caliphate Journal of Science & Technology, 1, 20-26.

Sahmoune, M. N. (2019). Evaluation of thermodynamic parameters for adsorption of heavy metals by green adsorbents. *Environmental Chemistry Letters*, *17*(2), 697-704.

Shaba, E. Y., Tijani, J. O., Jacob, J. O., and Suleiman, M. A. T. (2022). Simultaneous removal of Cu (II) and Cr (VI) ions from petroleum refinery wastewater using Fe_3O_4/ZnO nanocomposite. *Journal of Environmental Science and Health, Part A*, *57*(13-14), 1146-1167.

Shaba, E.Y., Mathew, J.T, Musah, M., and Agboba, E.I. (2019). The Kinetic and Thermodynamic Study of the Removal of Selected heavy Metals from a Nigerian Brewery Wastewater Using Activated Carbon From Cheese Wood (alstonia boonei). "Theme: Sustainable Energy in hanging limate: The Role of Science and Technology", in 2nd School of Physical Sciences Biennial International Conference Futminna 2019, on 24th -27th June, Minna, Niger State.

Sumaila A. Enenchel D. E. Mathew J. T. and Okaraga A. S. (2016). Synthesis and Characterization of Prymethamine-Sulphadoxine Metal Complexes. *African Journal of Science and Research.* 1(5), 63 – 66.

Thoda, O., Moschovi, A.M., Sakkas, K.M., Polyzou, E. and Yakoumis, I. (2023). Highly Active under VIS Light M/TiO2 Photocatalysts Prepared by Single-Step Synthesis. Applied Science, 13, 6858.

Wang, R., Deng, L., Fan, X., Li, K., Lu, H., and Li, W. (2021). Removal of heavy metal ion cobalt (II) from wastewater via adsorption method using microcrystalline cellulose–magnesium hydroxide. *International journal of biological macromolecules*, *189*, 607-617.

Zaimee, M. Z. A., Sarjadi, M. S., and Rahman, M. L. (2021). Heavy Metals Removal from Water by Efficient Adsorbents. *Water*, *13*(19), 2659